

Solder Joint Reliability Assessment for a High Performance RF Ceramic Package

Paul Charbonneau, Hans Ohman, Marc Fortin
Sanmina Corporation
500 Palladium Dr.
Ottawa, Ontario K2V 1C2 Canada
Ph: 613-886-6000; Fax: 613-886-6001
Email: paul.charbonneau@sanmina.com

Abstract

The prediction of long term solder joint reliability, (SJR), of microelectronic devices and packaging solutions continues to challenge the microelectronic packaging industry, particularly with the introduction of lead-free materials, the push for higher performance (frequency/speed/thermal) and lower unit cost. High performance packages are generally custom designed and therefore have minimal industry data on configuration specific reliability performance. In this application, the package substrate coefficient of thermal expansion, (CTE), was closely matched to the die resulting in a relatively large CTE mismatch between the package and organic PCB. In addition, the package RF and thermal performance requirements required this particular solution to be configured as a “cavity down” perimeter ball array with a large central ground pad to electrically couple the package to the PCB. Given the package’s unique design requirements and CTE mismatch, even modest daily temperature swings of 20°C usually found in a controlled or “Central Office” environment could have an adverse impact on the interconnect reliability.

This study provides an overview of the solder joint reliability assessment methodologies performed for a custom design lead-free, high performance RF package as part of the requirements to demonstrate compliance to product specifications. SJR life predictions were made for varying package BGA configurations using a multi-tiered approach using constitutive material models, thermo-mechanical finite element simulations, and material specific fatigue models. Empirical accelerated life testing was performed and a life prediction obtained through modeling was validated. Finally, statistical failure distributions were fit to empirical data and discussed in the context of absolute solder life predictions of small fractions unit failures, (100ppm).

Key words

Lead-free solder, Microelectronic packaging, RF packaging, RoHS compliant, Solder joint reliability, Weibull failure distribution

I. Introduction

Solder joint reliability prediction continues to be a critical aspect of a reliability assessment of microelectronic packages and electronic hardware and systems in general. Solder joint failure due to temperature cycling induced creep is considered the dominant failure mechanism in a “Central Office” environment. Coefficient of thermal expansion (CTE) mismatch between the package and printed circuit board (PCB), combined with temperature excursions due to assembly processing and daily ambient temperature cycling, result in solder joint stress, plastic strain and creep that cause cracking and ultimately the failure of the package to PCB solder interconnect. For SnPb solders, there is a significant amount of industry

data based on a relatively mature and broad range of electronic applications. This has supported the development of robust, empirically derived constitutive material models, failure prediction models, and acceleration factors that can predict solder joint life and allow for confidence in modeling and design. In the case of lead-free materials compliant to the Restriction of Hazardous Substances Directive, (RoHS), the general failure mechanism remains the same, however, sensitivities to stresses are different from those of lead containing solders. While constitutive material, failure prediction and acceleration models exist for lead-free solders, they are less mature and more work is required to build confidence in these models.

An additional complication to solder joint reliability analysis is the definition of product life requirements. Typically defined as a small fraction of unit failures under field conditions, predictions of this nature require assumptions or test data of failure rates/distributions to arrive at predictions for a small fraction of failures. Finally, translating model and test data to field use conditions requires acceleration factors that are empirically derived and material specific. Absolute mean life predictions have limited accuracy, [1], [2], and these compounding factors introduce additional uncertainty in a long term prediction. In this study, relative and absolute SJR life predictions were made for a high performance RF microelectronic package. Empirical studies were also performed to further assess reliability and validate SJR predictions.

II. Package Description

The package considered in this study is a ceramic, “cavity down” package with a top-side heat spreader, and bottom-side perimeter ball array and large central ground pad/lid. Fig. 1, 2a, and 2b show package size, configuration and overall dimensions.

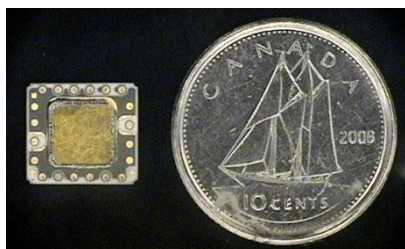


Figure 1: RF Package bottom view (BGA/ground pad/lid side up) with Canadian dime for size comparison

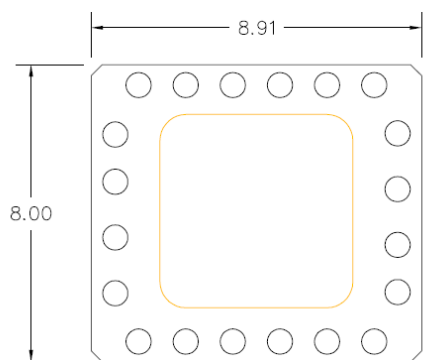


Figure 2a: Package bottom view (mm)

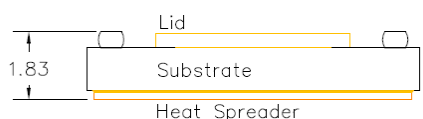


Figure 2b: Package side view (mm)

Given the difference in the CTE of the ceramic substrate and the application defined PCB, ($\Delta CTE_{\text{PCB-Substrate}} = 7.5\text{ppm}/^\circ\text{C}$), BGA balls in this configuration span a relatively large CTE mismatch compared with organic packages.

Solder balls of different sizes were considered as a design tradeoff between package solder joint reliability and RF performance; larger spheres are preferred for reliability while smaller spheres are preferred for performance. With respect to solder material, SAC305 was chosen based on 2nd level assembly requirements, therefore alternate SAC formulations were not considered.

III. Solder Life Prediction

A. Modeling Approach

A half-symmetry model of the package was created and simulations were run using ANSYS Static Structural FEA software. Collapsed BGA ball shapes were estimated using The Surface Evolver, an application for modeling liquid surfaces, [3]. Ball shapes were influenced by selections of initial ball diameter, pad diameter and stand-off height. Pad locations, and hence BGA pitch, were not varied for different ball configurations. A summary of the geometries considered is presented in Table 1, and a visual comparison of these geometries is shown in Fig. 3.

Table I – Modeled Ball Shape Parameters

Ball #	Initial Ball Diameter (mm)	Pad Diameter (mm)	Stand-off Height (mm)	Resultant Max Diameter (mm)	Height / Pad Diameter
1	0.61	0.55	0.44	0.68	0.80
2	0.50	0.46	0.37	0.57	0.80
3	0.51	0.50	0.36	0.58	0.73
4	0.41	0.40	0.31	0.47	0.78
5	0.38	0.37	0.29	0.45	0.80

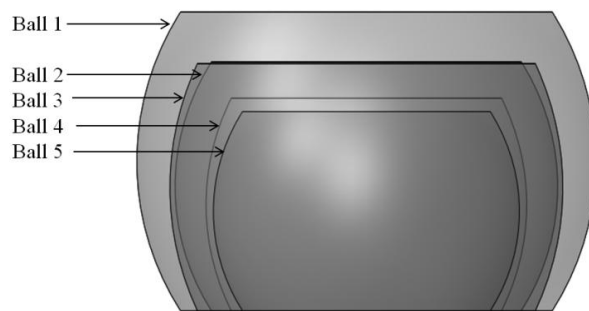


Figure 3: Resultant collapsed BGA ball shapes

To understand the impact of certain shape variables, additional shapes were considered by scaling the collapsed

0.6mm ball shape. Balls 2 and 5 described in Table 1 are scaled versions of Ball 1.

Package materials and the system level PCB material properties (CTE, Young's modulus and Poisson's ratio) were estimated and a constitutive model in the form of a double power law was used for the SAC305 BGA balls based on work by Wiese, Meusel and Wolter, [4].

The general life prediction approach used in this study is based on empirical correlations between simulation data and test data, performed by Syed, [2] and [5], with both accumulated creep strain and creep energy density used as failure metrics. A detailed/fine mesh was applied to the area of the critical solder joint, the ball farthest from the package centre. Both failure metrics were volume averaged over a 25 micron thick slice of the critical solder balls at the package and board interfaces. As per [5], a minimum of two elements were modeled across the thickness of the critical ball slices. An example meshed ball geometry is shown in Fig. 4.

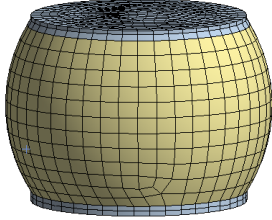


Figure 4: Sample BGA ball geometry / mesh

Simulations assumed the solder reflow temperature as the stress-free temperature of the package-PCB assembly. A thermal load simulated an accelerated thermal cycle so as to correlate with SJR testing and failure models presented by [5]. A cycle from 0°C to 100°C with 15min ramp rates and 15min dwells was used. Simulations were run for three complete thermal cycles and damage metrics were taken as the accumulated metric over the complete third thermal cycle.

Simulations were run on models with three different diameter BGA balls, (0.4mm, 0.5mm and 0.6mm), and sensitivities were explored by varying the ball/pad geometry, mesh density, material properties and boundary conditions.

As per [5], absolute mean life of the critical solder joint was estimated with (1) and (2):

$$N_f = (0.1968 \varepsilon_{acc})^{-1} \quad (1)$$

$$N_f = (0.0066 w_{acc})^{-1} \quad (2)$$

where,

N_f = mean number of cycles to failure,

ε_{acc} = accumulated creep strain per cycle, and

w_{acc} = accumulated creep strain energy density per cycle.

Note that (1) and (2) are specific to the double power law constitutive model for SAC305 from [4].

B. Modeling Results

In all cases the package-ball interface is predicted to be the location of failure. Normalized modeled mean life predictions are presented for both failure metrics in Fig. 5 and in Table II. The inelastic stain energy density failure model consistently predicts longer mean life than the inelastic strain failure model.

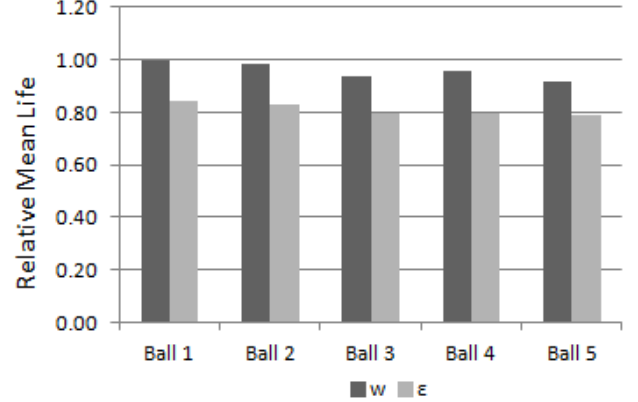


Figure 5: Normalized mean life (N_f) for different ball geometries based on accumulated creep strain, ε_{acc} , and creep energy density, w_{acc}

Table II – Normalized mean life (N_f) for different ball geometries

Ball #	N_f based on w_{acc}	N_f based on ε_{acc}	Stand-off Height (mm)	Height / Pad Diameter
1	1.00	0.84	0.44	0.80
2	0.99	0.83	0.37	0.80
3	0.94	0.79	0.36	0.73
4	0.96	0.80	0.31	0.78
5	0.92	0.79	0.29	0.80

Simulations predict Ball 1, the largest ball with the highest stand-off height, to be the most reliable configuration; however, less than a 10% difference is predicted in mean life across all configurations.

Simulation results show stand-off height to be an important variable with respect to solder joint reliability; however, pad diameter and the ratio of height to pad diameter are also found to be important variables. At roughly the same stand-off height, the more slender Ball 2 is predicted to be more reliable than Ball 3, which has a larger pad diameter.

As an isolated variable, stand-off height is predicted to have a non-linear relationship with reliability; Fig. 6 shows the relative reliability of similar shape balls, (proportionally scaled), plotted with respect to stand-off height.

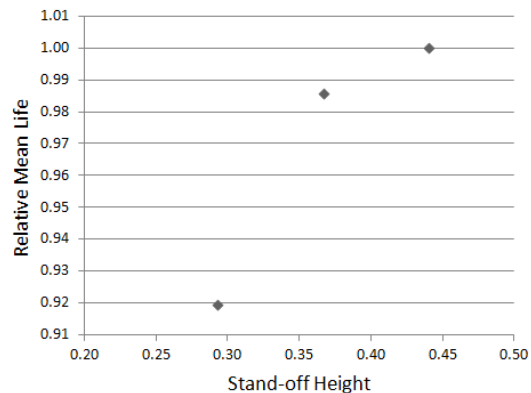


Figure 6: Relative reliability of balls with equal proportions at different stand-off heights; Balls 1, 2 and 5

C. Initial 100ppm Field Life Prediction

In considering package design with respect to the product's reliability requirements, modeling results were used to arrive at an absolute life prediction for the failure of 100ppm units in use in field conditions.

A product failure distribution had to be assumed to arrive at 100ppm life prediction estimates without test data. For this analysis, 2 parameter and 3 parameter, (2-p and 3-p), Weibull distributions were considered and „typical“ failure distribution parameters were used in calculations. In the case of a 2-p Weibull distribution, a shape parameter of 11 was assumed as per [2]. In the case of a 3-p Weibull distribution, the shape parameter was assumed to be 2.6 and the shift parameter was assumed to be half of the scale parameter, as per [1]. The validity of these assumptions is discussed later in this paper.

To arrive at an absolute life prediction for field-use conditions, a literature review was performed to determine an appropriate acceleration factor for SAC305 solder. Many empirically derived models have been presented in recent years and eight models were considered in this study, [6]–[11], providing a wide range of life estimates. The selection of an acceleration factor, however, is not discussed in this paper.

To summarize, the three major steps to determine the final life estimate were: a failure model to arrive at a mean life prediction; a failure distribution to arrive at 100ppm prediction; and, finally, an acceleration factor to arrive at field-use prediction. Given these compounding steps, absolute life predictions were initially made with upper and lower bounds, presented in Table III. These bounds reflect minimum and maximum life estimates for combinations of two failure models, two failure distributions and eight acceleration factors. Table III demonstrates the importance of selecting appropriate failure distributions and acceleration factors.

Table III – Absolute product life predictions in years

Ball #	Lower Bound	Life Prediction	Upper Bound
1	6	18	51

IV. Physical Testing

A. Test Setup

Given the nature of the product's reliability requirements and the uncertainty surrounding lead-free solder joint life predictions, validation testing was performed on packages with a „Ball 1“ configuration. A set of 32 daisy chained package assemblies were mounted to PCBs and temperature cycled in a single cavity chamber using the same regime simulated in life prediction modeling: 0°C to 100°C with 15min ramp rates and 15min dwells. The test PCB was designed to match dimensional and material properties of the PCB used in simulations and the product application (board thickness, stack up, material set, pad size, etc.). An event detector monitored in-situ resistance of all BGA balls connected in 4 discrete nets per package. The detector event threshold set at 300Ω and a unit was considered failed as per the recommended failure criteria laid out in [12].

B. Test Results

At the end of testing, 29 of the 32 test packages had experienced solder joint failure. Several units were cross-sectioned through the BGA and imaged using scanning electron microscopy, (SEM). BGA geometry was validated, and as predicted solder joint failures occurred at the package interface to the BGA ball, as seen in Fig. 7.

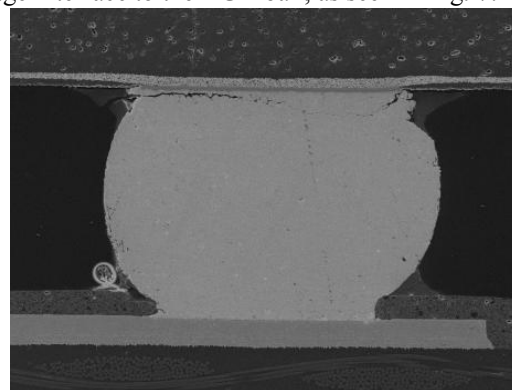


Figure 7: SEM image of cross-section of failed BGA ball

The failure data was fit to both 2-p and 3-p Weibull distributions. Fig. 8a and 8b show plots of SJR test data fitted with probability density function, (PDF), and cumulative distribution functions, (CDF), respectively.

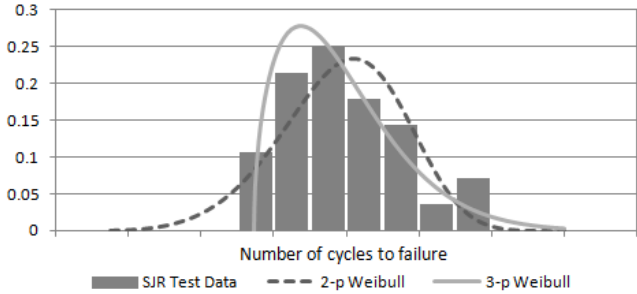


Figure 8a: PDF of test data fit with Weibull distributions

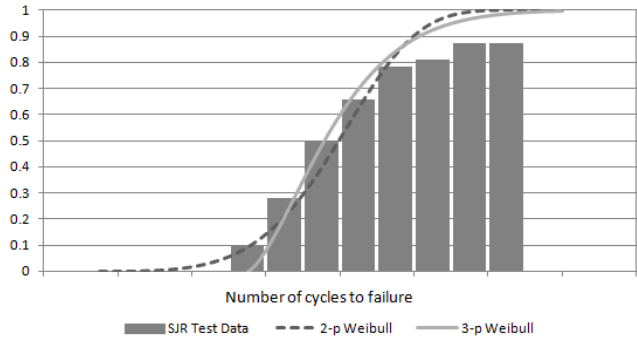


Figure 8b: CDF of test data fit with Weibull distributions

Using probability plot estimates, the 2-p distribution fit test data with a shape parameter of 5.24 and a „goodness of fit“, R-squared value of 0.8722. The 3-p distribution fit test data with a shape parameter of 1.5 and an R-squared value of 0.9948.

Looking qualitatively at the plots, the 2-p distribution has a long leading tail that affects the life prediction of a small fraction of failures significantly. Given the relatively low R-squared value and leading tail, this 2-p distribution may provide an overly-conservative estimate of 100ppm life. Conversely, the 3-p distribution fits the data very well, and while the large shift presumes a significant failure free life and provides a less conservative prediction of 100ppm life, the „goodness-of-fit“ of the 3-p distribution with test data warrants some consideration of failure-free life.

V. Comparison of Results

A comparison of fitted test data with simulated mean life estimates obtained from „Ball 1“ modeling is presented in Table IV.

Mean life predictions obtained from simulations fit well with test data, especially for the creep strain energy density failure model. The creep stain energy density model predicted a mean life 12% less than the mean life obtained from testing. The creep strain model was more conservative, with a mean life differing from test data by 25%.

Table IV – Simulated mean life predictions, normalized to test data fit with 2-p and 3-p Weibull distributions

		Test Data Variables	
		2-p fit	3-p fit
Model Variables	w_{acc}	0.88	0.88
	ϵ_{acc}	0.75	0.75

Looking back to initial assumed 100ppm life predictions, Figure 9 compares plots of test data fit with the „industry typical“ 2-p and 3-p Weibull parameters used to initially calculate 100ppm life estimates, with best fit distributions.

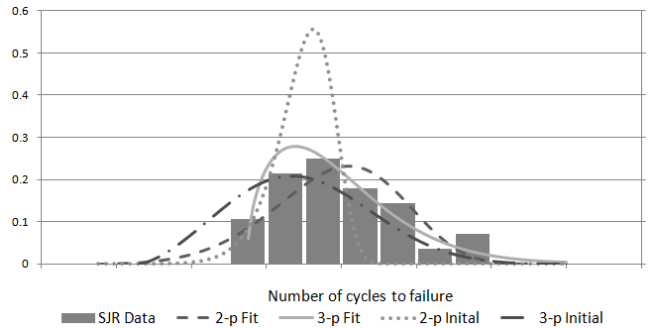


Figure 9a: PDF of test data fit with best fit and assumed Weibull parameters

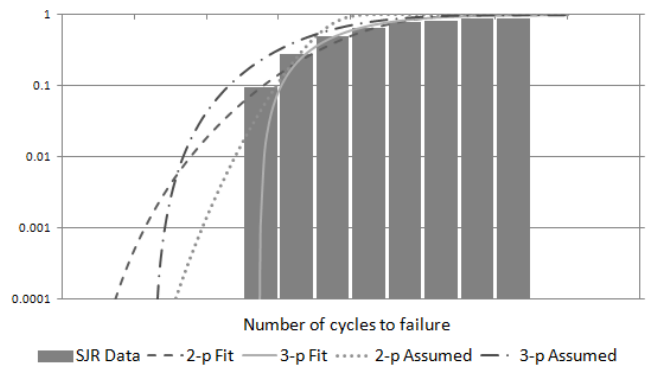


Figure 9b: CDF of test data fit with best fit and assumed Weibull parameters

A „typical“ 2-p Weibull shape parameters assumes a tighter failure distribution as the shape of the distribution does not fit the bulk of the data; however, the large shape parameter forces a large slope early in the distribution which forms a much less gradual leading tail.

With a lower shape parameter, the best fit 2-p distribution provides the most conservative 100ppm life estimate, the leading tail affecting estimates at low fractions.

Data fit with „typical“ 3-p Weibull parameters used the assumption that the shift parameter equaled half of the scale parameter and as such the entire distribution is shifted toward a lower life prediction. In this particular case the

assumption appears to be overly conservative. Most notable is that the 100ppm life predictions calculated using these distributions differ by as much as 5x. This highlights the importance of selecting an appropriate failure distribution when making predictions at small fractions of failures.

VI. Conclusion

An overview of the solder joint reliability assessment methodology for a custom design lead-free, high performance RF package has been presented, including:

- predictive modeling to estimate mean life,
- test data to estimate a failure distribution, and 100ppm life, and,
- an acceleration factor to estimate life under field-use conditions.

This reliability assessment was required to demonstrate compliance with product reliability specifications.

Modeling results showed that solder joint height, and pad size selections affect solder joint reliability. Future work will include the validation of these observations through additional solder joint testing for varying solder ball configurations (collapsed height and diameter).

Based on validation tests, the failure models proposed by Syed, [5], were found to provide reasonably accurate mean life predictions. The failure model based on accumulated inelastic strain energy density, w_{acc} , provided a mean life estimate 12% less than the best fit test data. The failure model based on inelastic strain, ε_{acc} , was more conservative, but still within 25% of the best fit test data.

The selection of an appropriate failure distribution was shown to be a critical element in making reasonable life predictions as it has a significant impact on estimates, especially when considering a small fraction of unit failures, (100ppm). Test data fit best to a 3 parameter Weibull distribution with a shift parameter representing failure-free life. The 3-p distribution precipitates a much less conservative 100ppm life prediction compared to a 2 parameter distribution. In this study the assumption of a 3-p distribution with a significant failure-free life seems valid given test data, but the topic warrants further investigation through additional empirical studies with larger sample sizes.

Acceleration factors were not explicitly discussed, however, several published models were considered in the analysis, [6]-[11], providing a range of acceleration factors that differed by as much as 4x for „Central Office“ conditions.

Ultimately, the assessment demonstrated the product solder joint reliability had sufficient margin to meet the required reliability specification. Additional modeling and validation tests on varying packages and solder joint configurations are required to further refine the selection of an appropriate

failure distribution and acceleration factor.

Acknowledgment

The authors would like to acknowledge and thank Mike Newhouse of Sanmina, and Denis Cousineau of the University of Ottawa for their comments.

References

- [1] R. Darveaux, "Effect of simulation methodology on solder joint crack growth correlation," *IEEE Electronic Components and Technology Conf.*, May 2000, pp. 1048-1058
- [2] A. Syed, "Accumulated creep strain and energy density based thermal fatigue life prediction models for SnAgCu solder joints" *IEEE Electronic Components and Technology Conf.*, June 2004, pp. 737-746 Vol. 1.
- [3] K. Brakke. (2013, August 25). The Surface Evolver (Ver. 2.7), [Online]. Available: www.susqu.edu/brakke/evolver/evolver.html
- [4] S. Wiese, E. Meusel and K-J Wolter, "Microstructural dependence of constitutive properties of eutectic SnAg and SnAgCu solders," *IEEE Electronic Components and Tech. Conf.*, May 2003, pp. 197-206.
- [5] A. Syed, "Updated life prediction models for solder joints with removal of modeling assumptions and effect of constitutive equations," *Thermal, Mechanical and Multiphysics Simulations and Experiments in Micro-Electronics and Micro-Systems Conf.* April 2006, pp. 1-9.
- [6] N. Pan, G.A Hensall, F. Billaut, "An acceleration model for Sn-Ag-Cu solder joint reliability under various thermal cycle conditions," *SMTA International Conf. Proc.*, 2006, pp. 876-883.
- [7] O. Salmela, "Acceleration factors for lead-free solder materials," *IEEE Trans. Components and Packaging Technologies*, vol. 30, Dec. 2007, pp. 700-707.
- [8] W. Dauksher, "A second-level SAC solder-joint fatigue-life prediction methodology," *IEEE Transactions on Device and Materials Reliability*, vol. 8, March 2008, pp. 168-173
- [9] V. Vasudevan, X. Fan, "An acceleration model for lead-free (SAC) solder joint reliability under thermal cycling," *IEEE Electronic Components and Technology Conference*, May 2008, pp. 139-145.
- [10] P. Lall, A. Shirgaokar, D. Arunachalam, "Principal component analysis based development of Norris-Landzberg acceleration factors and Goldmann constants for leadfree electronics," *IEEE Electronic Components and Technology Conference*, May 2009, pp. 251-261.
- [11] J-P. Clech, G. Henshall, J. Miremadi, "Closed-form, strain-energy based acceleration factors for thermal cycling of lead-free assemblies," *SMTA International Conf. Proc.* Oct. 2009
- [12] *Guidelines for Accelerated Reliability Testing of Surface Mount Solder Attachments*, IPC Standard, IPC-SM-785, 1992.
- [13] D. Cousineau, University of Ottawa, Ottawa, ON, private communication, March, 2014